Reconstruction of the arcuate fasciculus for surgical planning in the setting of peritumoral edema using two-tensor unscented Kalman filter tractography

The Harvard community has made this article openly available. Please share how this access benefits you. Your story matters

Citation	Chen, Zhenrui, Yanmei Tie, Olutayo Olubiyi, Laura Rigolo, Alireza Mehrtash, Isaiah Norton, Ofer Pasternak, Yogesh Rathi, Alexandra J. Golby, and Lauren J. O'Donnell. 2015. "Reconstruction of the arcuate fasciculus for surgical planning in the setting of peritumoral edema using two-tensor unscented Kalman filter tractography." NeuroImage : Clinical 7 (1): 815-822. doi:10.1016/j.nicl.2015.03.009. http://dx.doi.org/10.1016/j.nicl.2015.03.009.
Published Version	doi:10.1016/j.nicl.2015.03.009
Citable link	http://nrs.harvard.edu/urn-3:HUL.InstRepos:17295720
Terms of Use	This article was downloaded from Harvard University's DASH repository, and is made available under the terms and conditions applicable to Other Posted Material, as set forth at http://nrs.harvard.edu/urn-3:HUL.InstRepos:dash.current.terms-of-use#LAA

CrossMark

Reconstruction of the arcuate fasciculus for surgical planning in the setting of peritumoral edema using two-tensor unscented Kalman filter tractography

Zhenrui Chen[a,d], Yanmei Tie[a], Olutayo Olubiyi[a], Laura Rigolo[a,b], Alireza Mehrtash[a,b], Isaiah Norton[a], Ofer Pasternak[b,c], Yogesh Rathi[c], Alexandra J. Golby[a,b,*,1], Lauren J. O'Donnell[a,b,**,1]

[a]Department of Neurosurgery, Brigham and Women's Hospital, Harvard Medical School, Boston, MA 02115, USA
[b]Department of Radiology, Brigham and Women's Hospital, Harvard Medical School, Boston, MA 02115, USA
[c]Department of Psychiatry, Brigham and Women's Hospital, Harvard Medical School, Boston, MA 02115, USA
[d]Department of Neurosurgery, Jinling Hospital, Southern Medical University, Nanjing, Jiangsu 210002, China

ARTICLE INFO

ABSTRACT

Background: Diffusion imaging tractography is increasingly used to trace critical fiber tracts in brain tumor patients to reduce the risk of post-operative neurological deficit. However, the effects of peritumoral edema pose a challenge to conventional tractography using the standard diffusion tensor model. The aim of this study was to present a novel technique using a two-tensor unscented Kalman filter (UKF) algorithm to track the arcuate fasciculus (AF) in brain tumor patients with peritumoral edema.

Methods: Ten right-handed patients with left-sided brain tumors in the vicinity of language-related cortex and evidence of significant peritumoral edema were retrospectively selected for the study. All patients underwent 3-Tesla magnetic resonance imaging (MRI) including a diffusion-weighted dataset with 31 directions. Fiber tractography was performed using both single-tensor streamline and two-tensor UKF tractography. A two-regions-of-interest approach was applied to perform the delineation of the AF. Results from the two different tractography algorithms were compared visually and quantitatively.

Results: Using single-tensor streamline tractography, the AF appeared disrupted in four patients and contained few fibers in the remaining six patients. Two-tensor UKF tractography delineated an AF that traversed edematous brain areas in all patients. The volume of the AF was significantly larger on two-tensor UKF than on single-tensor streamline tractography (p < 0.01).

Conclusions: Two-tensor UKF tractography provides the ability to trace a larger volume AF than single-tensor streamline tractography in the setting of peritumoral edema in brain tumor patients.

1. Introduction

The purpose of brain tumor surgery is to achieve maximal lesion removal while maintaining or improving neurological function. For brain tumor resection, it is important to identify the key white matter tracts pre- or intra-operatively to avoid damaging them during surgery (Elhawary et al., 2011; Nimsky et al., 2007). Diffusion tensor imaging (DTI) tractography provides an innovative tool for investigating white matter architecture in vivo (Tournier et al., 2011). The use of this technique has been increasing in neurological surgery in recent years (Liu et al., 2011; Castellano et al., 2012). However, the effects of peritumoral edema pose a major challenge to conventional DTI tractography when tracing fiber tracts that are adjacent to malignant tumors (Zhang et al., 2013; Schonberg et al., 2006; Kinoshita et al., 2005). Peritumoral edema is usually related to dysfunction of the blood brain barrier that causes fluid to leak into the extracellular space, resulting in image voxels that contain part cerebral parenchyma and part extracellular water (Pasternak et al., 2009). DTI tractography (Basser et al., 2000), while robust, uses a single-tensor model that is inadequate in the case of partial volume, crossing fibers, and edema (Nimsky, 2014; Duffau, 2014).

In patients with brain tumors in the vicinity of language areas, definition of the relationship between language pathways and the surgical lesion becomes important. Classically thought to connect anterior

(Broca's) and posterior (Wernicke's) language regions, the arcuate fasciculus (AF) is a C-shaped structure that connects temporal, parietal, and frontal lobes (Catani and Mesulam, 2008). The AF is arguably the most significant white matter fiber tract associated with language function, although there is some debate over the precise functional deficit that may accompany damage to it (Dick and Tremblay, 2012), as well as over the relationship of standard DTI tractography of the AF with functional areas. In a study using cortical stimulation for language mapping in focal epilepsy, DTI tractography of the AF colocalized well with Broca's areas but less so with Wernicke's areas (Diehl et al., 2010), while in another study, it was noted that DTI tractography connected to motor and premotor areas rather than to Broca's anterior language area (Bernal and Ardila, 2009). Thus in the clinical context, tracing of the AF poses a challenge.

To improve fiber tracking, it is becoming accepted that methods must move beyond the diffusion tensor (Nimsky, 2014; Farquharson et al., 2013; Fernandez-Miranda, 2013). Identifying a robust model to interpret the diffusion signal is thus of importance. In addition to modeling, the method chosen for tractography is still an open question in the diffusion neuroimaging analysis field (Jbabdi and Johansen-Berg, 2011), thus it is important to test tractography methods in clinical data, including in patients with brain tumors and edema. In this work, we evaluated the two-tensor unscented Kalman filter (UKF) tractography framework (Malcolm et al., 2010), where a two-tensor model is fit to the underlying data during the process of fiber tracking. The UKF tractography method was initially designed for neuroscientific studies, such as detection of abnormalities in first-episode schizophrenia (Rathi et al., 2011). In contrast to other methods that fit a model to the signal independently at each voxel (Qazi et al., 2009), in the UKF framework (Wan and Van Der Merwe, 2000) each tracking step employs prior information from the previous step to help fit and stabilize the model. The concept of employing information from the previous step during tracking (in an earlier DTI-based approach called tensor deflection; Lazar et al., 2003; Weinstein et al., 1999; Westin et al., 2002) has been shown to improve neurosurgical tractography (Feigl et al., 2014). In healthy subject data, it has been shown that for clinically typical diffusion data (b-value near 1000 s/mm^2), two-tensor UKF tractography outperforms other models such as spherical harmonics in terms of tractography coverage of expected connections (Baumgartner et al., 2012).

The aim of this study was to determine whether two-tensor UKF tractography could improve the tracking of AF in brain tumor patients with peritumoral edema.

2. Materials and methods

2.1. Patient selection

We retrospectively evaluated all consecutive brain tumor patients who had undergone functional MRI and diffusion imaging through December 2008 and June 2012 at Brigham and Women's Hospital. Patients were selected for inclusion if they met the following criteria: (1) Brain tumor patients with peritumoral edema in the vicinity of the language

cortex; (2) patients were native English speakers and right-handed as determined by the Edinburgh Handiness Inventory (Oldfield, 1971); (3) patients were left-hemisphere dominant for language according to functional MRI results. Exclusion criterion: The reconstructed AF did not pass through the peritumoral edema. In this study, a total of 126 brain tumor patients who had undergone functional and diffusion imaging were identified. 13 of these patients met the inclusion criteria, and after AF reconstruction 3 of the 13 met the exclusion criteria. After the exclusion of ineligible subjects, the study included 10 patients (4 male, 6 female; age range 37–77 years). We note that our initial goal was to include at least 10 subjects in the study; this goal was achieved by evaluating consecutive patients up to June 2012. Detailed patient demographics, including clinical presentation, tumor histology and tumor localization, are detailed in Table 1. The study was approved by the Partners Healthcare Institutional Review Board, and informed consent was obtained from all participants prior to scanning.

2.2. MRI acquisition

MR images were obtained using a 3-Tesla scanner (EXCITE Signa scanner, GE Medical System, Milwaukee, WI, USA) with Excite 14.0, using an 8-channel head coil and array spatial sensitivity encoding technique (ASSET). High resolution whole brain T1-weighted axial 3D spoiled gradient recalled structural images (TR = 7500 ms, TE = 30 ms, matrix = 512 × 512, FOV = 25.6 cm, flip angle = 20°, 176 slices, voxel size = 0.5 × 0.5 × 1 mm^3) were acquired. Diffusion weighted images were acquired using EPI with 8 channel head coil and ASSET (TR = 14,000 ms, TE = 75.4, 31 gradient directions evenly distributed on the sphere, b-value of 1000 s/mm^2, 1 baseline image, FOV = 25.6 cm, matrix = 128 × 128, 44 slices, voxel size = 2 × 2 × 3 mm^3). Acquisition of structural, diffusion, and functional imaging datasets took 45–60 min per patient.

2.3. Preprocessing of DTI data

3D Slicer (http://www.slicer.org, version 4) was used to convert the raw data from DICOM format into NRRD format (Gering et al., 2001). DTIPrep (http://www.nitrc.org/projects/dtiprep) was used to perform quality control (Liu et al., 2010), which included artifact correction/removal as well as eddy-current and head motion artifacts correction by registration to the baseline image. In 3D Slicer, fractional anisotropy (FA) maps were created and the standard color scheme was used to visualize the DTI eigenvector orientations (with blue indicating superior–inferior, red indicating transverse, and green indicating anterior–posterior) and brightness controlled by FA. Then, both single-tensor streamline and two-tensor UKF tractography were applied to each diffusion MRI dataset.

2.4. Single-tensor streamline tractography

For each dataset, a binary brain mask was computed in 3D Slicer from the diffusion images to restrict tractography (see below) to within

Table 1
Patient demographics.

Patient	Age (years)	Sex	Presentation	Pathology	Localization
1	54	F	Facial twitching, word-finding difficulties	Glioblastoma multiform, WHO IV	Fronto-parietal
2	37	M	Seizures, word-finding difficulties	Recurrent oligodendroglioma, WHO II	Frontal
3	77	M	Slurred speech, word-finding difficulties	Glioblastoma multiform, WHO IV	Temporo-parietal
4	56	F	Headaches, word-finding difficulties	Glioblastoma multiform, WHO IV	Temporal
5	48	F	Headaches, speech difficulties	Glioblastoma multiform, WHO IV	Parieto-occipital
6	44	M	Slurred speech, abnormal facial movement	Anaplastic oligodendroglioma, WHO III	Frontal
7	64	F	Sub-acute aphasia	Glioblastoma multiform, WHO IV	Temporal
8	41	F	Headaches, word-finding difficulties	Anaplastic oligodendroglioma, WHO III	Frontal
9	43	M	Seizures	Glioblastoma multiform, WHO IV	Temporal
10	60	F	Facial twitching, speech arrest	Atypical meningioma, WHO II	Frontal

WHO, World Health Organization.

the brain. Single-tensor streamline tractography was performed in the 3D Slicer using the second-order Runge–Kutta (midpoint) method. Whole brain tractography was seeded within the brain mask in all voxels where single tensor FA was greater than 0.15. Tractography stopped when FA fell below 0.15.

2.5. Two-tensor UKF tractography

First proposed by Malcolm et al. (2010), the two-tensor UKF algorithm performs simultaneous fiber model estimation and neural tractography. In this method, the signal is modeled as a mixture of two tensors, and tractography is performed within a filtering framework. Starting from a seed point, each fiber is traced to its termination using UKF to simultaneously fit the local model to the signal and subsequently propagate in the most consistent direction.

The two-tensor UKF tractography was conducted in high performance computing clusters (HPC) and used to trace whole brain fiber tracts. As in single tensor tractography (above), the tractography was seeded within the binary brain mask in all voxels where single tensor FA was greater than 0.15, and tractography stopped when FA (of the tensor being tracked) fell below 0.15. In addition to the FA thresholds, the UKF method uses an additional value, the generalized anisotropy (GA), to further restrict tracking to regions where a two-tensor fit is reasonable. Based on the variance of normalized diffusivities, GA is sensitive to the presence of anisotropic structure such as that of fiber crossings. The GA threshold for seeding is always 0.18 in the UKF method. The GA was also employed as an additional stopping criterion, and we used the default value of 0.10. The results from whole brain tractography based on the two-tensor UKF algorithm were imported into 3D Slicer for further analysis.

2.6. Fiber bundle selection

Fiber bundle selection was performed in the 3D Slicer platform. A two-ROI approach was employed in the selection of the AF (Wakana et al., 2004). The specific ROIs were determined by a clinically trained neurosurgical research fellow (Z.C.) based on the color-coded FA map and structural images. A coronal slice at the level of the pre-central gyrus was chosen for drawing the first ROI (Catani and Thiebaut de Schotten, 2008). The author manually defined the ROI that encompassed all green voxels lateral to the blue corona radiata (Kamali et al., 2014). The second ROI was drawn on the axial slice at the level of the anterior commissure and encompassed all the posterior periventricular blue voxels (Kamali et al., 2014). Nearby isotropic voxels were included if these regions were affected by peritumoral edema. Using an "AND" operation, the fiber bundle that passed through the two ROIs was tracked. No waypoint or exclusion masks were used.

If the single-tensor streamline whole brain tractography, combined with the two-ROI fiber bundle selection, failed to detect any fiber tract, the Tractography Fiducial Seeding module (Golby et al., 2011), which employs the single-tensor streamline algorithm in 3D Slicer, was used as an alternative tool to track potentially disrupted AFs. The tool's interactive fiber tracking enabled detection of shorter fibers that did not reach both ROIs. For visualization of fiber tracts overlaid on anatomy, diffusion baseline images were automatically registered to structural images using the General Registration (BRAINS) module (Johnson et al., 2007) in 3D Slicer and manually checked to confirm appropriate registration.

2.7. Volume measurement of the AF

The measurement of the AF volume is a proxy for "connection strength" or "connection completeness" and is very commonly performed in studies using tractography (Forkel et al., 2014; Fletcher et al., 2010; Propper et al., 2010; Matsumoto et al., 2008; Li et al., 2013; Halwani et al., 2011). The Fiber Bundle to Label Map module in 3D Slicer was used to transform the AF into a label map (a segmented image volume, in this case a binary mask). This module sets a specified label value in the label map at every vertex of each of the fibers in each AF. Then, the Label Statistics module was applied to calculate the label volume. The volume of the AF was defined as the volume of the voxels occupied by the fibers in each subject (Propper et al., 2010).

2.8. Statistical analysis

Statistical analysis was performed using STATA (version 11.0; StataCorp, College Station, TX, USA). Standard summary statistics were used to describe the volume measurement data. Paired t-tests were used to compare means across tractography methods. A value of $p < .05$ (two-tailed) was considered statistically significant.

3. Results

The single-tensor streamline and two-tensor UKF fiber tractography results were compared visually and quantitatively, and the evaluation of the AF was based on knowledge of neuroanatomy. When using single-tensor streamline tractography, the AF appeared disrupted in four of ten patients, while the remaining six patients displayed thin fiber bundles. In contrast, the two-tensor UKF tractography produced an AF that appeared anatomically intact in all ten patients. In general, the two-tensor UKF tractography provided the ability to trace the AF more fully than the single-tensor streamline tractography in the setting of peritumoral edema. The procedure for single-tensor streamline whole brain tractography took 5–10 min on a desktop computer while two-tensor UKF tractography required up to 20 min for a single subject in the HPC.

3.1. Case illustration

We have illustrated the differences in four selected cases (Figs. 1–4).

3.1.1. Patient 1

Fig. 1 shows images from patient 1 who presented with episodes of facial twitching and word-finding difficulties. T2-weighted fluid-attenuated inversion recovery MRI showed an extensive inhomogeneous lesion at the left frontal parietal junction. The region of T2 prolongation extended to the parietal white matter as well as the internal and external capsule (Fig. 1A). The lesion showed inhomogeneous enhancement after injection of Gd-DTPA (Fig. 1B). The enhancing region extended fairly deep into the left hemisphere.

Fig. 1C and D presents axial and coronal views of the color-coded FA maps respectively. The AF appeared disrupted (shown by the arrows in Fig. 1C and D) by edema when compared with the healthy hemisphere.

In this patient, we found that the single-tensor streamline whole brain tractography combined with two-ROI approach failed to display the AF. Then, fiducial-based interactive tractography was used to track the potentially disrupted AF. Fig. 1E and G shows that fiducial-based interactive tractography tracked few frontally located fibers (yellow) near the tumor (green surface model). No temporal fibers were traced using fiducial-based interactive tractography.

In contrast, two-tensor UKF tractography (red) demonstrated a frontotemporally arching fiber bundle (Fig. 1F and H). The temporal projections of the fiber tracts reached the superior, middle and inferior temporal gyri, while the frontal projections reached the pars opercularis, pars triangularis and the middle frontal gyrus. The results from the two-tensor UKF tractography corresponded to the usual anatomical descriptions of the AF (Catani and Mesulam, 2008; Dick and Tremblay, 2012).

3.1.2. Patient 2

Fig. 2 shows images from patient 2, a 37-year-old male who presented with seizures, word finding difficulties and short-term memory problems. He was originally diagnosed with a left frontal oligodendroglioma and
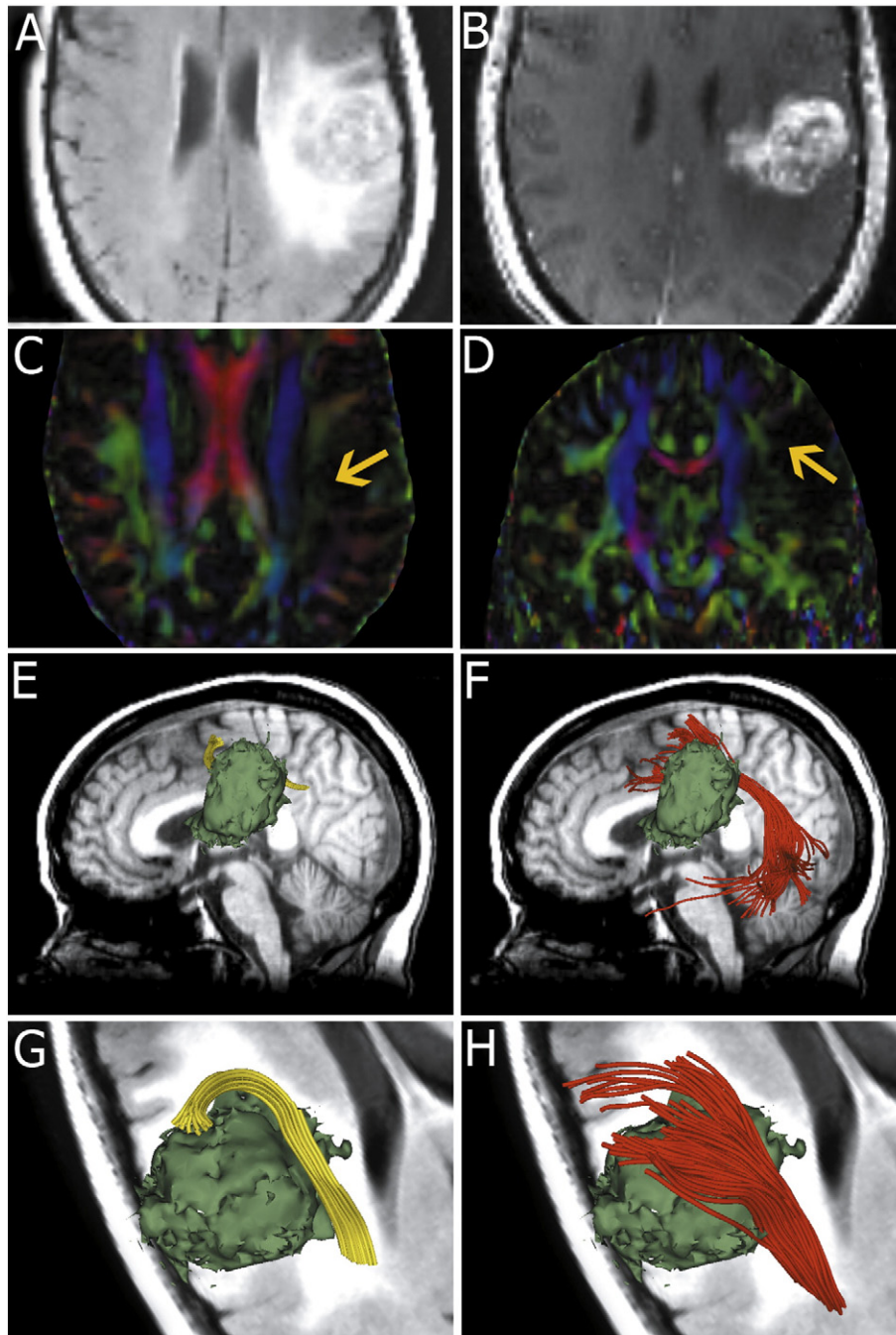
Fig. 1. Images from patient 1 with a left fronto-parietal lesion. Fluid-attenuated inversion recovery image demonstrates extensive edema around the lesion (A). T1-weighted postcontrast image shows a fronto-parietal junction tumor with significant enhancement (B). Color-coded FA maps (C and D) appear to indicate the AF is disrupted by peritumoral edema (arrows). Single tensor model reconstruction of the AF (yellow) fails to track the fiber tracts that run through the edematous area (E and G) near the tumor (green model). However, two-tensor unscented Kalman filter (UKF) tractography (red) shows that the temporal projections of the fiber tracts reach the superior, middle and inferior temporal gyri and the frontal projections reach the pars opercularis, pars triangularis and the middle frontal gyrus (F and H).

underwent surgical resection in 2002 and 2004. He was followed up with serial scans and there was evidence of radiographic progression in 2010. Fig. 2A and C shows that single-tensor streamline tractography did not trace through the edema (arrow). However, the two-tensor UKF method depicted fibers passing through the peritumoral edema (Fig. 2B and D, arrow).

3.1.3. Patient 4

Fig. 3 demonstrates images from patient 4, who presented with left-sided headaches and developed word-finding difficulties. Axial thin-slice T2-weighted images showed a 3.5 cm mass lesion (green surface model) in the left lateral temporal lobe close to the temporo-parietal junction, with surrounding white matter edema extending to the posterior aspect of the left internal and external capsules. Fig. 3A shows the fiber trajectory reconstructed by single-tensor streamline tractography. This image appears to show a disrupted AF, terminating in the peritumoral edema margin in the vicinity of the supramarginal gyrus (arrow). However, two-tensor UKF tractography delineated frontotemporally arching fibers running through the T2-bright area (Fig. 3B, arrow). 3D lateral views of the results from two different
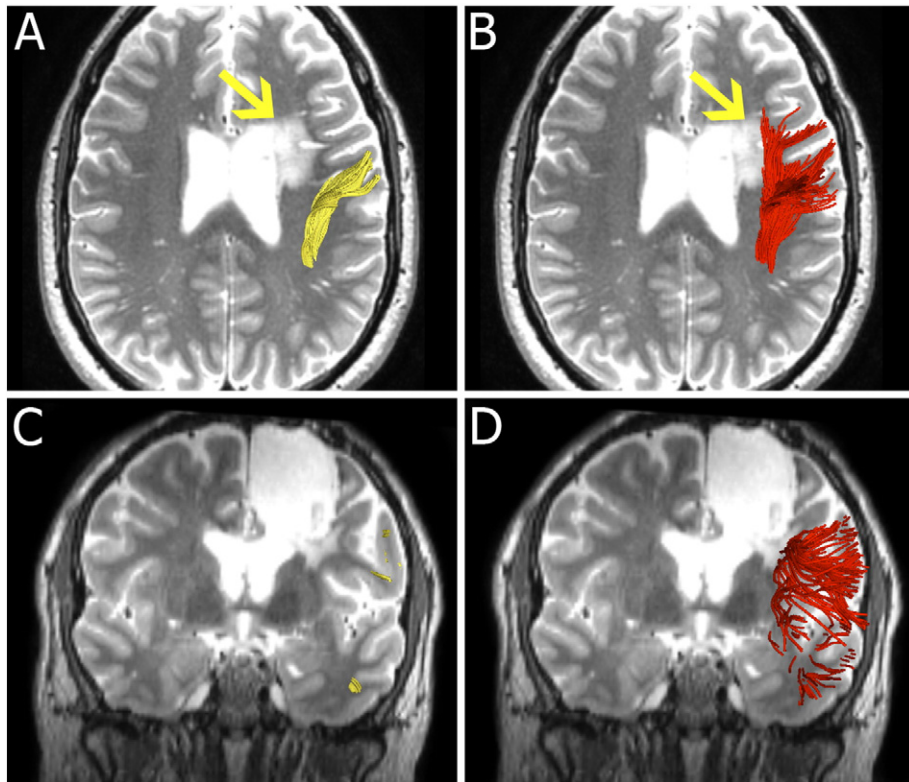
Fig. 2. Images from patient 2 with recurrent oligodendroglioma (A and C, arrow). Single-tensor streamline tractography fails to track the portion of AF going through the edema (B and D, arrow). Two-tensor UKF tractography depicts an intact AF, successfully tracking through the peritumoral edema.

methods are illustrated in Fig. 4C and D. Single-tensor streamline tractography displayed a small frontal fiber bundle (Fig. 3C) while two-tensor UKF tractography output a larger and longer fiber bundle, particularly displaying the arc around the Sylvian fissure (Fig. 3D).

3.1.4. Patient 8

Fig. 4 shows images from patient 8, who presented with headaches and word finding difficulty. Axial and coronal T2-weighted images (Fig. 4A and B respectively) show an abnormal area of T2 prolongation
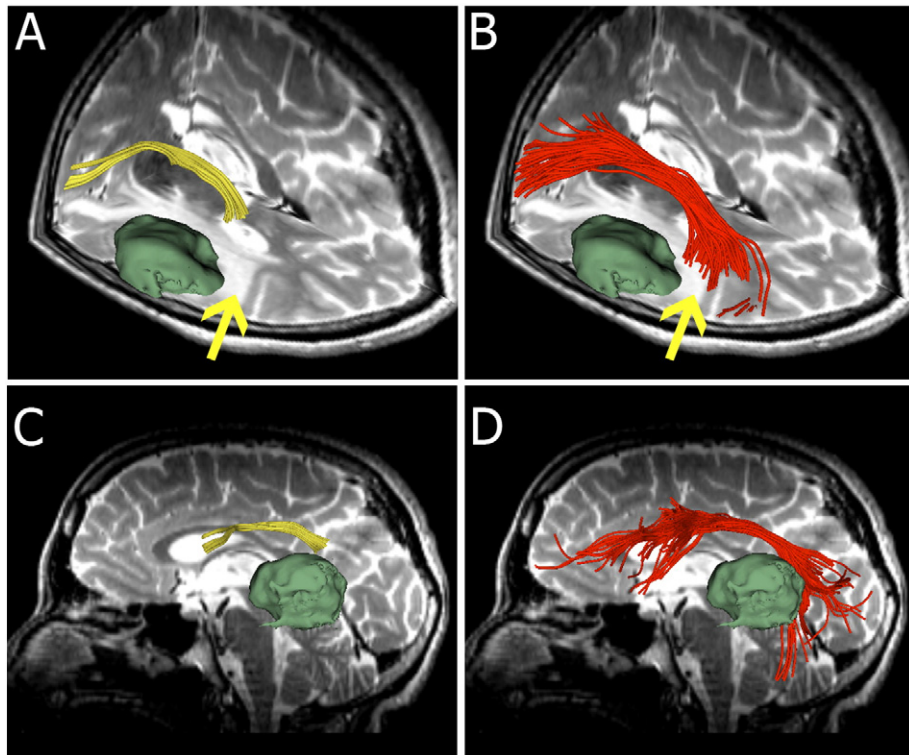

Fig. 3. Images from patient 4. (A and C) Single-tensor streamline tractography (yellow) appears to indicate a disrupted AF, terminating in the vicinity of the peritumoral edema margin (arrow). (B and D) Two-tensor UKF tractography produces a frontotemporally arching tract running through the T2-bright area (arrow).
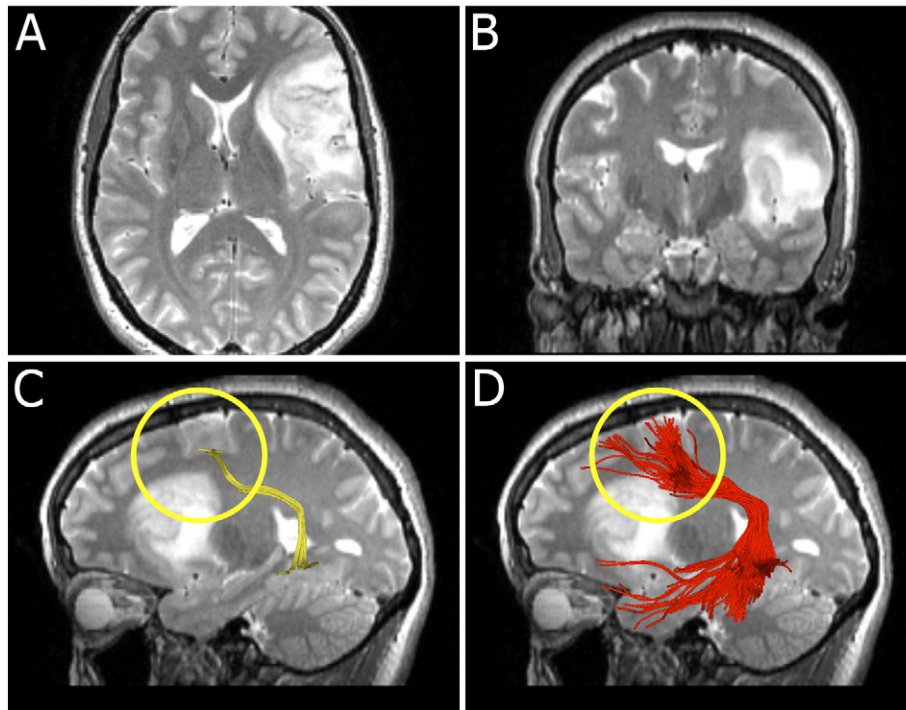
Fig. 4. Images from patient 8 who presented with word-finding difficulties. Axial (A) and coronal (B) T2-weighted images show a lesion involving the left frontal lobe, the left insula, the left external capsule and the anterior left temporal lobe. We highlight the frontal part of AF (circled). (C) Single-tensor streamline tractography tracks a small fiber bundle posterior to the tumor. (D) Two-tensor UKF tractography tracks the AF through the edematous area, adjacent to the tumor.

involving the left frontal lobe, the left insula, the left external capsule and the anterior left temporal lobe. Fig. 4C and D highlights the reconstruction of the frontal part of the AF (circled) from the two different algorithms. Single-tensor streamline tractography produced a thin fiber bundle behind the tumor (Fig. 4C). A fuller depiction of the AF was apparent using two-tensor UKF tractography (Fig. 4D).

3.2. Volume analysis

The volumes of the AF from two-tensor UKF tractography were significantly greater than those from the single-tensor streamline tractography method (Fig. 5). In our patient dataset, the single-tensor streamline group mean (SD) left AF volume in mm^3 was 2201.9 (2294.7), while the two-tensor UKF group mean (SD) left AF volume in mm^3 was 11,685.4 (6970.9), two-tailed $p < 0.01$.
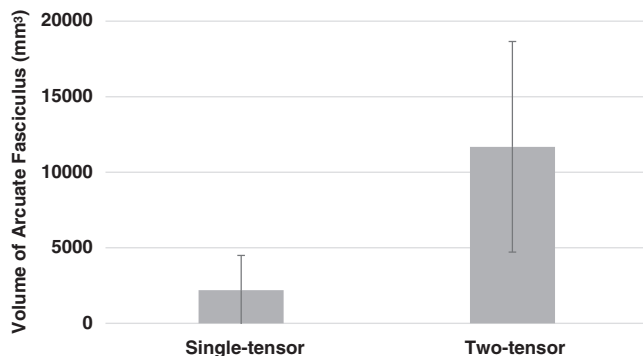

Fig. 5. Bar graph showing a significant difference between the volumes of the arcuate fasciculi as measured by single-tensor streamline and two-tensor UKF tractography methods, n = 10, $p < 0.01$, two-tailed paired t-test.

4. Discussion

Our results show that two-tensor UKF tractography traces a larger volume of AF than single-tensor streamline tractography in the setting of peritumoral edema. In the ten patients studied, the two-tensor UKF tractography reconstructed AF was consistent with the expected anatomy of the AF (Catani and Mesulam, 2008; Dick and Tremblay, 2012).

It is important to note that the performance of two-tensor UKF tractography in tracing the AF in our study may be partly due to its ability to improve the mapping in areas of crossing fibers. In healthy controls, anatomical studies of the AF have been performed using methods for modeling crossing fibers. For example, a study using data with a b-value of 1000 and probabilistic tractography demonstrated multiple frontal and temporal connections of AF (Rilling et al., 2008), while another study, performed using q-ball high b-value imaging, found the AF connected instead to areas superior to Broca's (Frey et al., 2008). In related work, O'Donnell et al. (2013) demonstrated that fibers passing through the putative Wernicke's activation robustly reached the putative Broca's activation only with the two-tensor UKF model in a healthy subject, when compared to single-tensor methods. Though there is debate about the precise connections made by the AF (Dick and Tremblay, 2012), it is clear that accounting for fiber crossings is important.

Other studies have also proposed analysis and/or acquisition methods to improve tracking of the AF through edema or crossing fibers in neurosurgical patient data. Kuhnt et al. (2013) demonstrated that compressed sensing could be used to reconstruct high angular resolution (HARDI) fiber models and improve tracking of the AF in neurosurgical patients. Both our study and theirs were performed using similar clinical scans of around 30 directions at a b-value of 1000 s/mm^2, and acquisition times under 15 min. Their study was not specifically focused on edema, however they did report improved fiber tracking in those patients with edema. In contrast to our study, they employed sharpened spherical harmonics to model the fiber orientations at each voxel (Descoteaux et al., 2009), a method that, in a recent comparison,

produced less-complete coverage than two-tensor UKF in terms of fiber tract endpoints reaching expected anatomical areas (Baumgartner et al., 2012). The results of both studies indicate that the standard b-value for routine clinical imaging (b = 1000 s/mm^2) may be sufficient for tracing the AF, when combined with sophisticated processing. Another study by Zhang et al. (2013) employed standard clinical b = 1000 s/mm^2 data (with 25 directions), but applied generalized q-sampling reconstruction (a method expected to be applicable only for high b-value multiple shell data). Some limited improvements were found in edematous regions.

Others have investigated the problem of edema by modeling diffusion compartments or free water. McDonald et al. (2013) used high b-value restriction spectrum imaging data to estimate tensors corresponding to the restricted diffusion compartment, a part of the model that was not expected to include edema. Pasternak et al. (2009) proposed an algorithm that estimates free water from diffusion MRI obtained by conventional DTI acquisitions, enabling better estimation of FA in areas of partial volume effect near ventricles, or in edema. The free water model is a second tensor that is isotropic, with eigenvalues equal to the diffusivity of free water. In contrast, the two-tensor UKF model used in this study employs two five-parameter tensors (where there are five instead of six parameters because the smaller two eigenvalues are modeled as equal) (Malcolm et al., 2010). In our experiments presented here, the two-tensor model appeared flexible enough to model the edema in addition to any crossing fibers affecting the AF, and in future studies it would be of interest to test the combined two-tensor model and the free-water model within the UKF framework.

Fiber tracking in the setting of peritumoral edema is of particular interest for neurosurgical planning for resection of tumors with significant edema. It would benefit neurosurgeons to be aware that if conventional DTI tractography cannot trace the AF through edema, it does not mean that the AF is totally destroyed, particularly for patients without apparent language functional impairment. However, increased sensitivity for tracking anatomical structures has the potential to influence surgery to be more conservative, in the sense that less tissue may be removed. In general, it is best for the surgeon to have the most accurate information possible and then make a judgment about what the meaning of that information is.

It is worth noting that high grade tumors are very aggressive pathological processes and the peritumoral T2 signal change can be attributed not only to increased water content, but also to tumor cell infiltration. The extent of tumor cell infiltration is difficult to define based on imaging (Eis et al., 1994). Because our current study includes only one high-grade glioma patient, the current results cannot be interpreted as relating to infiltration. Rather, they demonstrate only that UKF tractography could improve tracking through regions of edema.

We measured volume, which does not directly indicate that the AF is functional, is connected to language areas, or is healthy. However, it does indicate what spatial extent of the tract was able to be traced by each algorithm, and it is a popular anatomical tract measure for AF research (Forkel et al., 2014; Fletcher et al., 2010; Propper et al., 2010; Matsumoto et al., 2008; Li et al., 2013; Halwani et al., 2011). The volume of the AF has been shown to relate to clinical outcomes, such as aphasia recovery (Forkel et al., 2014). Thus the AF volume is a relevant parameter for comparison of tractography methods.

The potential for false positives is an important consideration with all tractography methods (Ciccarelli et al., 2008). The current manuscript focuses more on the issue of avoiding potential false negatives, such as when a tract cannot be traced (Zhang et al., 2013). There are many ways to fit a diffusion or fiber model to the data, and the biexponential model fit used in UKF is not a unique solution, however the method does fit the data with very low error. It is important to clarify that the UKF method does not in fact "bypass" any data; it uses the prior model fit as an initial condition for fitting the model to the data at a new location. It takes many small steps within each voxel so that the model adapts to the local data. The UKF method does fit the data with very low error, however issues such as partial voluming (Lazar

et al., 2003) or the topic of this study, edema, are known to reduce confidence in fiber tract orientations (Assaf and Pasternak, 2008).

Although this study shows obvious advantages regarding two-tensor UKF tractography, certain limitations of the study should be mentioned. First, the two-tensor UKF tractography algorithm is more computationally intensive than the single-tensor streamline tractography approach, so the execution time of the method is greater and it requires more computational resources. When tested on a regular desktop computer (Intel®Xeon CPU 3.10 GHz × 4; 15.6 GiB Memory; 2014), it took 22–30 min to run per patient. Second, although the two-tensor tractography technique appears to be much more robust than the single-tensor technique, considering that there is no gold standard for validation, the possibility of false positives should be taken into account. Thus the neurosurgeon should carefully interpret the results of tractography in the context of anatomical knowledge. Third, an important line of research is to validate preoperative fiber tracking with the aid of intraoperative stimulation, such as the subcortical stimulation used recently for motor tract validation (Mandelli et al., 2014). However, intraoperative subcortical stimulation is not used routinely in our department and was not available for this retrospective study. Fourth, diffusion imaging and tractography are not able to differentiate between functional and nonfunctional tracts, nor between purely edematous versus infiltrated tracts. Finally, the UKF two-tensor model is not a biophysical model, and as such, there is no edema-specific model. Future work will assess the effect of a free-water model, an additional tensor with diffusivity fixed to that of free water, in tracking through edema. However, as this free water tensor is spherical, it is not expected to have a large impact on estimation of fiber orientations; rather it may improve the other tensor fits by decreasing the influence of edema (Pasternak et al., 2009).

5. Conclusion

Diffusion imaging tractography is increasingly used to trace critical fiber tracts in brain tumor patients. We have demonstrated that the two-tensor UKF tractography method can trace a larger volume AF than single-tensor streamline tractography in the setting of peritumoral edema. Although the two-tensor UKF tractography algorithm shows promise in reconstruction of the AF for neurosurgical planning, the method is still under active development and requires further validation.

Conflicts of interest

The authors have no conflicts of interest to report.

Acknowledgments

References

Assaf, Y., Pasternak, O., 2008. Diffusion tensor imaging (DTI)-based white matter mapping in brain research: a review. J. Mol. Neurosci. 34 (1), 51–61. http://dx.doi.org/10.1007/s12031-007-0029-018157658.

Basser, P.J., Pajevic, S., Pierpaoli, C., Duda, J., Aldroubi, A., 2000. In vivo fiber tractography using DT-MRI data. Magn. Reson. Med. 44 (4), 625–632. http://dx.doi.org/10.1002/1522-2594(200010)44:4<625::AID-MRM17>3.0.CO;2-O11025519.

Baumgartner, C., Michailovich, O., Levitt, J., et al., 2012. A Unified Tractography Framework for Comparing Diffusion Models on Clinical Scans at: CDMRI Workshop-MICCAI, Nice.

Bernal, B., Ardila, A., 2009. The role of the arcuate fasciculus in conduction aphasia. Brain J. Neurol. 132 (9), 2309–2316. http://dx.doi.org/10.1093/brain/awp20619690094.

Castellano, A., Bello, L., Michelozzi, C., et al., 2012. Role of diffusion tensor magnetic resonance tractography in predicting the extent of resection in glioma surgery. Neuro-Oncology 14 (2), 192–202. http://dx.doi.org/10.1093/neuonc/nor18822015596.

Catani, M., Mesulam, M., 2008. The arcuate fasciculus and the disconnection theme in language and aphasia: history and current state. Cortex J. Devoted Study Nerv. Syst. Behav. 44 (8), 953–961. http://dx.doi.org/10.1016/j.cortex.2008.04.00218614162.

Catani, M., Thiebaut de Schotten, M., 2008. A diffusion tensor imaging tractography atlas for virtual in vivo dissections. Cortex J. Devoted Study Nerv. Syst. Behav. 44 (8), 1105–1132. http://dx.doi.org/10.1016/j.cortex.2008.05.00418619589.

Ciccarelli, O., Catani, M., Johansen-Berg, H., Clark, C., Thompson, A., 2008. Diffusion-based tractography in neurological disorders: concepts, applications, and future developments. Lancet Neurol. 7 (8), 715–727. http://dx.doi.org/10.1016/S1474-4422(08)70163-718635020.

Descoteaux, M., Deriche, R., Knösche, T.R., Anwander, A., 2009. Deterministic and probabilistic tractography based on complex fibre orientation distributions. I. E.E.E. Transactions Med. Imaging 28 (2), 269–286. http://dx.doi.org/10.1109/TMI.2008.200442419188114.

Dick, A.S., Tremblay, P., 2012. Beyond the arcuate fasciculus: consensus and controversy in the connectional anatomy of language. Brain J. Neurol. 135 (12), 3529–3550. http://dx.doi.org/10.1093/brain/aws22223107648.

Diehl, B., Piao, Z., Tkach, J., et al., 2010. Cortical stimulation for language mapping in focal epilepsy: correlations with tractography of the arcuate fasciculus. Epilepsia 51 (4), 639–646. http://dx.doi.org/10.1111/j.1528-1167.2009.02421.x20002151.

Duffau, H., 2014. The dangers of magnetic resonance imaging diffusion tensor tractography in brain surgery. World Neurosurg. 81 (1), 56–58. http://dx.doi.org/10.1016/j.wneu.2013.01.11623376386.

Eis, M., Els, T., Hoehn-Berlage, M., Hossmann, K.A., 1994. Quantitative diffusion MR imaging of cerebral tumor and edema. Acta Neurochir. Suppl. (Wien) 60 (Suppl.), 344–3467976585.

Elhawary, H., Liu, H., Patel, P., et al., 2011. Intraoperative real-time querying of white matter tracts during frameless stereotactic neuronavigation. Neurosurgery 68 (2), 506–516. http://dx.doi.org/10.1227/NEU.0b013e318203628221135719.

Farquharson, S., Tournier, J.D., Calamante, F., et al., 2013. White matter fiber tractography: why we need to move beyond DTI. J. Neurosurg. 118 (6), 1367–1377. http://dx.doi.org/10.3171/2013.2.JNS121294235402169.

Feigl, G.C., Hiergeist, W., Fellner, C., et al., 2014. Magnetic resonance imaging diffusion tensor tractography: evaluation of anatomic accuracy of different fiber tracking software packages. World Neurosurg. 81 (1), 144–150. http://dx.doi.org/10.1016/j.wneu.2013.01.00423295636.

Fernandez-Miranda, J.C., 2013. Editorial: beyond diffusion tensor imaging. J. Neurosurg. 118 (6), 1363–1365. http://dx.doi.org/10.3171/2012.10.JNS12180023540267.

Fletcher, P.T., Whitaker, R.T., Tao, R., et al., 2010. Microstructural connectivity of the arcuate fasciculus in adolescents with high-functioning autism. Neuroimage 51 (3), 1117–1125. http://dx.doi.org/10.1016/j.neuroimage.2010.01.08320132894.

Forkel, S.J., Thiebaut de Schotten, M., Dell'Acqua, F., et al., 2014. Anatomical predictors of aphasia recovery: a tractography study of bilateral perisylvian language networks. Brain J. Neurol. 137 (7), 2027–2039. http://dx.doi.org/10.1093/brain/awu11324951631.

Frey, S., Campbell, J.S., Pike, G.B., Petrides, M., 2008. Dissociating the human language pathways with high angular resolution diffusion fiber tractography. J. Neurosci. 28 (45), 11435–11444. http://dx.doi.org/10.1523/JNEUROSCI.2388-08.200818987180.

Gering, D.T., Nabavi, A., Kikinis, R., et al., 2001. An integrated visualization system for surgical planning and guidance using image fusion and an open MR. J Magn Reson Imaging 13 (6), 967–975. http://dx.doi.org/10.1002/jmri.113911382961.

Golby, A.J., Kindlmann, G., Norton, I., Yarmarkovich, A., Pieper, S., Kikinis, R., 2011. Interactive diffusion tensor tractography visualization for neurosurgical planning. Neurosurgery 68 (2), 496–505. http://dx.doi.org/10.1227/NEU.0b013e3182061ebb21135713.

Halwani, G.F., Loui, P., Rüber, T., Schlaug, G., 2011. Effects of practice and experience on the arcuate fasciculus: comparing singers, instrumentalists, and non-musicians. Front. Psychol. 2, 156. http://dx.doi.org/10.3389/fpsyg.2011.0015621779271.

Jbabdi, S., Johansen-Berg, H., 2011. Tractography: where do we go from here? Brain Connectivity 1 (3), 169–183. http://dx.doi.org/10.1089/brain.2011.003322433046.

Johnson, H., Harris, G., Williams, K., 2007. BRAINSFit: mutual information rigid registrations of whole-brain 3D images, using the insight toolkit. Insight J. http://hdl.handle.net/1926/1291.

Kamali, A., Flanders, A.E., Brody, J., Hunter, J.V., Hasan, K.M., 2014. Tracing superior longitudinal fasciculus connectivity in the human brain using high resolution diffusion tensor tractography. Brain Struct. Funct. http://dx.doi.org/10.1007/s00429-012-0498-y23288254.

Kinoshita, M., Yamada, K., Hashimoto, N., et al., 2005. Fiber-tracking does not accurately estimate size of fiber bundle in pathological condition: initial neurosurgical experience using neuronavigation and subcortical white matter stimulation. Neuroimage 25 (2), 424–429. http://dx.doi.org/10.1016/j.neuroimage.2004.07.07615784421.

Kuhnt, D., Bauer, M.H., Egger, J., et al., 2013. Fiber tractography based on diffusion tensor imaging compared with high-angular-resolution diffusion imaging with compressed sensing: initial experience. Neurosurg. 72 (Suppl. 1), 165–175. http://dx.doi.org/10.1227/NEU.0b013e318270d9fb23254805.

Lazar, M., Weinstein, D.M., Tsuruda, J.S., et al., 2003. White matter tractography using diffusion tensor deflection. Hum. Brain Mapp. 18 (4), 306–321. http://dx.doi.org/10.1002/hbm.1010212632468.

Li, Z., Peck, K.K., Brennan, N.P., et al., 2013. Diffusion tensor tractography of the arcuate fasciculus in patients with brain tumors: comparison between deterministic and probabilistic models. J. Biomed. Sci. Eng. 6 (2), 192–200. http://dx.doi.org/10.4236/jbise.2013.6202325328583.

Liu, X., Tian, W., Kolar, B., et al., 2011. MR diffusion tensor and perfusion-weighted imaging in preoperative grading of supratentorial nonenhancing gliomas. Neuro-Oncology 13 (4), 447–455. http://dx.doi.org/10.1093/neuonc/noq19721297125.

Liu, Z., Wang, Y., Gerig, G., et al., 2010. Quality control of diffusion weighted images. Proc Soc Photo Opt Instrum Eng 7628. http://dx.doi.org/10.1117/12.84474824353379.

Malcolm, J.G., Shenton, M.E., Rathi, Y., 2010. Filtered multitensor tractography. I. E.E.E. Transactions Med. Imaging 29 (9), 1664–1675. http://dx.doi.org/10.1109/TMI.2010.204812120805043.

Mandelli, M.L., Berger, M.S., Bucci, M., Berman, J.I., Amirbekian, B., Henry, R.G., 2014. Quantifying accuracy and precision of diffusion MR tractography of the corticospinal tract in brain tumors. J. Neurosurg. 121 (2), 349–358. http://dx.doi.org/10.3171/2014.4.JNS13116024905560.

Matsumoto, R., Okada, T., Mikuni, N., et al., 2008. Hemispheric asymmetry of the arcuate fasciculus: a preliminary diffusion tensor tractography study in patients with unilateral language dominance defined by Wada test. J. Neurol. 255 (11), 1703–1711. http://dx.doi.org/10.1007/s00415-008-0005-918821045.

McDonald, C.R., White, N.S., Farid, N., et al., 2013. Recovery of white matter tracts in regions of peritumoral FLAIR hyperintensity with use of restriction spectrum imaging. A.J.N.R. Am. J. Neuroradiol. 34 (6), 1157–1163. http://dx.doi.org/10.3174/ajnr.A337223275591.

Nimsky, C., 2014. Fiber tracking—we should move beyond diffusion tensor imaging. World Neurosurg. http://dx.doi.org/10.1016/j.wneu.2013.08.03524007693.

Nimsky, C., Ganslandt, O., Hastreiter, P., et al., 2007. Preoperative and intraoperative diffusion tensor imaging-based fiber tracking in glioma surgery. Neurosurgery 61 (1 Suppl.), 178–185. http://dx.doi.org/10.1227/01.neu.0000279214.00139.3b18813171.

O'Donnell, L.J., Golby, A.J., Westin, C.F., 2013. Fiber clustering versus the parcellation-based connectome. Neuroimage 80, 283–289. http://dx.doi.org/10.1016/j.neuroimage.2013.04.06623613987.

Oldfield, R.C., 1971. The assessment and analysis of handedness: the Edinburgh inventory. Neuropsychologia 9 (1), 97–113. http://dx.doi.org/10.1016/0028-3932(71)90067-45146491.

Pasternak, O., Sochen, N., Gur, Y., Intrator, N., Assaf, Y., 2009. Free water elimination and mapping from diffusion MRI. Magn. Reson. Med. 62 (3), 717–730. http://dx.doi.org/10.1002/mrm.2205519623619.

Propper, R.E., O'Donnell, L.J., Whalen, S., et al., 2010. A combined fMRI and DTI examination of functional language lateralization and arcuate fasciculus structure: effects of degree versus direction of hand preference. Brain Cogn. 73 (2), 85–92. http://dx.doi.org/10.1016/j.bandc.2010.03.00420378231.

Qazi, A.A., Radmanesh, A., O'Donnell, L., et al., 2009. Resolving crossings in the corticospinal tract by two-tensor streamline tractography: method and clinical assessment using fMRI. Neuroimage 47 (Suppl. 2), T98–T106. http://dx.doi.org/10.1016/j.neuroimage.2008.06.03418657622.

Rathi, Y., Kubicki, M., Bouix, S., et al., 2011. Statistical analysis of fiber bundles using multitensor tractography: application to first-episode schizophrenia. Magn. Reson. Imaging 29 (4), 507–515. http://dx.doi.org/10.1016/j.mri.2010.10.05521277725.

Rilling, J.K., Glasser, M.F., Preuss, T.M., et al., 2008. The evolution of the arcuate fasciculus revealed with comparative DTI. Nat. Neurosci. 11 (4), 426–428. http://dx.doi.org/10.1038/nn207218344993.

Schonberg, T., Pianka, P., Hendler, T., Pasternak, O., Assaf, Y., 2006. Characterization of displaced white matter by brain tumors using combined DTI and fMRI. Neuroimage 30 (4), 1100–1111. http://dx.doi.org/10.1016/j.neuroimage.2005.11.01516427322.

Tournier, J.D., Mori, S., Leemans, A., 2011. Diffusion tensor imaging and beyond. Magn. Reson. Med. 65 (6), 1532–1556. http://dx.doi.org/10.1002/mrm.2292421469191.

Wakana, S., Jiang, H., Nagae-Poetscher, L.M., van Zijl, P.C., Mori, S., 2004. Fiber tract-based atlas of human white matter anatomy. Radiology 230 (1), 77–87. http://dx.doi.org/10.1148/radiol.230102164014645885.

Wan, E.A., Van Der Merwe, R., 2000. The Unscented Kalman Filter for Nonlinear Estimation at: Adaptive Systems for Signal Processing, Communications, and Control Symposium. AS-SPCC. The IEEE 2000.

Weinstein, D., Kindlmann, G., Lundberg, E., 1999. Tensorlines: Advection-diffusion Based Propagation Through Diffusion Tensor Fields at: Proceedings of the Conference on Visualization'99: Celebrating Ten Years.

Westin, C.F., Maier, S.E., Mamata, H., Nabavi, A., Jolesz, F.A., Kikinis, R., 2002. Processing and visualization for diffusion tensor MRI. Med. Image Anal. 6 (2), 93–108. http://dx.doi.org/10.1016/S1361-8415(02)00053-112044998.

Zhang, H., Wang, Y., Lu, T., et al., 2013. Differences between generalized q-sampling imaging and diffusion tensor imaging in the preoperative visualization of the nerve fiber tracts within peritumoral edema in brain. Neurosurg. 73 (6), 1044–1053. http://dx.doi.org/10.1227/NEU.0000000000000014624056318.